Model predictive control for a medium-head hydropower plant hybridized with battery energy storage to reduce penstock fatigue

Stefano Cassano, Fabrizio Sossan

Model Predictive Control for a Medium-head Hydropower Plant Hybridized with Battery Energy Storage to Reduce Penstock Fatigue

Stefano Cassano, Fabrizio Sossan
MINES ParisTech, Université PSL, Centre Procédés Energies Renouvelables et Systèmes Energétiques (PERSEE)
Sophia Antipolis, France
{stefano.cassano, fabrizio.sossan}@mines-paristech.fr

***Abstract*—A hybrid hydropower power plant is a conventional Hydro-Power Plant (HPP) augmented with a Battery Energy Storage System (BESS) to decrease the wear of sensitive mechanical components and improve the reliability and regulation performance of the plant. A central task of controlling a hybrid HPP is determining how the total power setpoint is split between the BESS and the hydraulic turbine (power setpoint splitting). This paper describes a Model Predictive Control (MPC) framework for hybrid medium- and high-head HPPs for the power setpoint splitting problem. The splitting policy relies on an explicit formulation of the mechanical loads incurred by the HPP's penstock, which can be damaged due to fatigue when providing grid frequency regulation. By filtering out from the HPP's power setpoint the components conducive to excess penstock fatigue and properly controlling the BESS, the proposed MPC maintains the same level of regulation performance while significantly decreasing damages to the hydraulic conduits. A proof-of-concept by simulations is provided considering a 230 MW medium-head plant.**

***Index Terms*—Hybrid Power Plants, Battery Energy Storage System, Control, Hydropower plants.**

I. Introduction

Hydropower is a crucial asset of the electrical power system infrastructure, providing a significant amount of electricity and regulation services to the power grid. In 2018 hydropower accounted for 16.8% of the total European power production and 70% of all renewable generation [1].

The increasing proportion of stochastic generation in the electric power system will require steeper ramping duties and more frequent start-and-stops to all dispatchable generation units for grid balancing. Increased regulation duties for Hydro-Power Plants (HPPs) will lead to increased maintenance needs due to more wear and tear effects, negatively affecting plants' economics. More specifically, in medium- and high-head HPPs, steep changes of the plant's power setpoint result in hydraulic transients and water hammers in the hydraulic conduits (or penstocks), posing serious damage risks, as demonstrated in [2]. In low-head (or run-of-the-river) HPPs, increased regulation duties result in increased wear of the guide vane bushes and fatigue in the Kaplan turbine's blade actuator (e.g., [3]). Wearing is a severe concern for HPP operators because it leads to expensive maintenance which requires to take the plant off-grid for long periods.

A solution advocated in the technical literature to limit damaging the mechanical components and increase the reliability and flexibility of an HPP is adding, in parallel to the hydraulic turbine, a Battery Energy Storage System (BESS) to supply fast variations of the power output. This configuration is known as a hybrid HPP and can extend to other kinds of power plants (e.g., PV plants) and control objectives (e.g., improving dispatch). Hybridization came to prominence thanks to the decreasing prices of BESSs, especially Lithium-ion batteries, which can supply quick variations of power because of their fast kinetics, lack of mechanical time constants, and power-electronic interface. The notion of hybrid power plants is that operating the conventional plant and BESS within a unified control framework brings benefits over operating the two units separately, thanks to leveraging SCADA information or plant specificities that would not be otherwise available outside plant premises. This is valid especially for fatigue reduction, where required control actions are on a time scale of a few seconds, and specific plant information, such as power setpoints and speed governor properties, and measurements are needed.

The central objective of a hybrid HPP's control problem is that of computing how the power setpoint is shared among the two controllable resources, as exemplified in Fig. 1 for the BESS and the hydraulic turbine . We call this the *power setpoint splitting* problem, or *splitting* problem.

Addressing meaningful splitting policies targeting fatigue

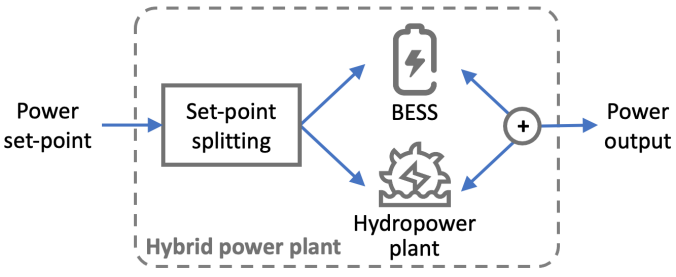

Fig. 1. A hybrid hydropower plant.

reduction in HPPs is a relatively new research problem, which has been addressed in the literature with empirical models so far. A commonly proposed strategy is low-pass filtering the power setpoint: the filtered setpoint is sent to the HPP for actuation, and the BESS takes the remaining part of the setpoint ([4], [5]). There are two main assumptions underlying this approach. The first is that high-frequency variations of the power setpoint are the root cause of fatigue in mechanical components; second, it assumes the existence of a formal procedure to translate from fatigue requirements to the cut-off frequency of the filter. However, both these assumptions are hard to be justified and realized in practice. In particular, because the fatigue and mechanical loads acting on the components are not modeled explicitly, low-pass filtering might result in conservative or wrong estimates of the fatigue level, ultimately resulting in excess use of the BESS, or be ineffective due to poor approximations and oversimplification of the wearing process.

For the first time in the literature, this paper proposes a splitting strategy for a hybrid HPP that explicitly models the impact of mechanical loads on fatigue. The method is based on Model Predictive Control (MPC). Unlike empirical methods that are uninformed of the actual fatigue levels of the mechanical components, the proposed MPC model the stress and fatigue of the penstock formally and explicitly, tackling the power splitting problem in a measurable and quantifiable way. This is thanks to (linearized) models of the mechanical loads in the penstock used to derive a closed-form expression for constraining the mechanical stress below the fatigue limit of the component.

The rest of this paper is organized as follows. Section II illustrates the problem, Section III describes the hybrid controller, Section IV discusses simulation results and the impact of modeling approximations introduced for the MPC, and Section V concludes the paper.

II. Problem statement

The principle of fatigue is that accumulated cycles of alternating mechanical loads (forces) on a component ultimately lead to ruptures and failure. In medium- and high-head HPPs, rapid variations of the power setpoint (as for primary and secondary frequency control) result in water hammers and pressure fluctuations within the penstock and are the root cause of penstock damages [2].

The central objective of the proposed hybrid HPP's controller is, first, adjusting the setpoint of the HPP to limit the water hammer, thus preserving the penstock from fatigue and avoiding expensive maintenance, and, second, using the BESS to compensate for the missing regulating power from the HPP.

The first component of this controller is an MPC that, by modeling the forces acting on the penstock walls resulting from a change of plant's power setpoint, removes those setpoint's components conducive to excess fatigue. This MPC, originally described [6], is summarized in III-C for the sake of clarity. Once the filtered setpoint is computed by the MPC, the BESS setpoint is computed as the difference from the original

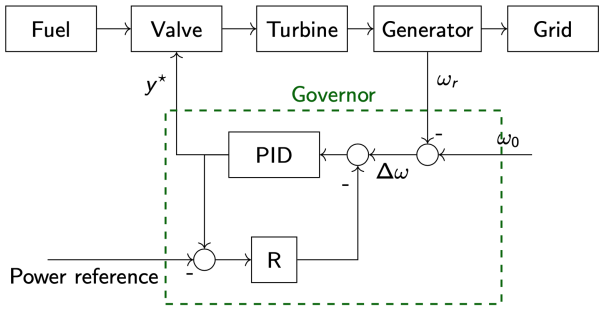

Fig. 2. Governor of a hydropower plant.

control setpoint: this stands as the central contribution of this paper and is described in III-D.

This paper assumes, for simplicity, an HPP with one turbine and one penstock. However, the methodology is general and, provided with the specific plant models, can be extended to accommodate other setups.

It is illustrative to discuss the standard regulation loop, or governor, of an HPP, which is shown in Fig. 2. The feedback loop on the rotor speed, ω_r, implements a frequency droop controller, where R is the droop coefficient, whose task is keeping the rotational speed of the machine near a design value, ω_0. The PID controller computes the position of the so-called *guide vane*, indicated by $y^\star$, which adjusts the flow of water to the turbine. The PID controller's parameters (which also include a ramp limiter, actuators' dynamics, and saturation limits, not shown here for compactness) are chosen to meet the response time requirements for grid frequency regulation, as exemplified in the Results section. Finally, the input signal *Power reference* is the speed changer setting that the operator uses to change the plant power setpoint for, e.g., secondary frequency regulation setpoints, rescheduling, etc.

The symbol $y^\star$ denotes the guide vane computed by the governor (Fig. 2). $y^\star$ is tuned to respect the static design limits of the plant. It is, however, uninformed of mechanical load dynamics in the penstock and fatigue effects. In particular, it might be conducive to premature aging if the power reference or the grid frequency signal requires frequent adjustments to the plant power output. Starting from $y^\star$, the proposed MPC computes a new guide vane setpoint that is cognizant of the dynamic stress constraints of the penstock.

It is worth highlighting that the current paper focuses only on penstock aging and not BESS aging. This is based on the assumption that the cost of maintaining (or replacing) a critical piece of infrastructure like the penstock is much larger than aging a BESS. This hypothesis is preliminarily corroborated by the findings of this paper, which show that the BESS power rating and energy capacity required to limit the penstock's fatigue is a small fraction of the plant's rated power; thus, BESS costs might be small. Aspects related to cycle aging of the BESS, which is, however, of definite general interest, will be investigated in future research to verify how the control action can also impact minimally on BESS residual life, as done, e.g., in [7], [8] in other contexts.

III. Controller of the hybrid hydropower plant

This section describes the formulation of the controller of the hybrid HPP. Beforehand, all the necessary modeling elements are summarized.

A. Modeling of hydropower plants

HPP models for power systems studies are typically transfer function and equivalent circuit models. They are also referred to as one-dimensional models, as opposed to computational fluid dynamic models in 2 or 3 dimensions, typically used to simulate the detailed behavior of a single hydraulic component and generally not suited to power systems simulations due to their computational complexity.

The equivalent circuit analogy consists in modeling the piezometric head (or head, measured in meters of water column), and volumetric flow rate (liter per second), at a given point of a hydraulic circuit as a voltage and current of an electrical circuit [9]. The equivalent circuit model of a medium-head HPP is shown in Fig. 3. It describes the water's flow rate and pressures within the hydraulic circuit of the plant. Its circuit elements are described in the following.

Voltage sources H_u and H_d are the head of the upstream and downstream reservoir;

The RLC circuits model the penstock. The penstock model is derived by applying water's momentum and mass conservation laws to an hydraulic conduit, assuming a one-directional flow along the longitudinal dimension. This results in a set of hyperbolic partial differential equations (PDEs) that, similarly to transmission lines' models [10], can be solved numerically by discretizing the spatial dimension in a finite number of elements $i = , 1, \dots, \mathcal{I}$. Each element i is a T-shaped third-order RLC circuit (Fig. 3), where the voltage h_i is the water head, and Q_i and Q_{i+1} are the volumetric flow rates at the receiving and sending ends at that penstock element i. This model captures head losses along the conduit and, most importantly, pressure dynamics within the penstock, which are at the origin of the water hammer effect. The circuit parameters can be inferred from penstock physical characteristics (e.g., [11]).

The inductor L_t models the inertia effect of the water in the turbine (where subscript t refers here to the hydraulic turbine).

The controlled voltage source $H_t(Q_t, \omega, y)$ models the head of a Francis turbine H_t as a function of rotational speed flow rate Q_t, rotation speed ω, and guide vane opening y. This model is derived from the turbine's head characteristic curve, which is computed experimentally from measurements. The turbine's characteristic model is generally nonlinear and assumes that the transient behavior of the turbine's head can be simulated as a succession of different steady-state operating points ("quasi-static" model). It ensures sufficient accuracy for all the flow regimes and tractable computational times [11].

It is worth highlighting that the hydraulic circuit of high-head power plants typically includes a surge tank too, which, although not discussed here, can be modeled using the same equivalent circuit principles.

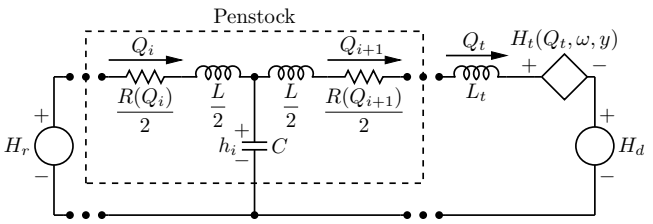

Fig. 3. Equivalent circuit model of the hydraulic circuit of a medium-head hydropower plant.

A second characteristic curve of the turbine, denoted by $T_t(Q_t, \omega, y)$, models the turbine's torque. The torque model, along with the equivalent circuit just described, constitutes the global dynamic model of the plant. Solving the model allows for computing all the HPP's state variables of the plant relevant for power system simulations.

B. Plant linearized model

The hydraulic circuit model in Fig. 3 and turbine's head and torque models H_t and T_t are nonlinear ([1]).

Under the assumption that the plant's setpoint and conditions do not change significantly within a few control periods (several seconds), a linearization can be achieved by modeling the penstock's resistance as a constant value, and the turbine's head and torque with a first-order Taylor approximation [12]. For the sake of illustration, the linear model of the head $\widetilde{H}$ is:

$$\begin{aligned}\widetilde{H}_t(Q_t, \omega, y) \approx H_t(Q_{t_0}, \omega_0, y_0) + d_Q^H \cdot (Q_t - Q_{t_0}) + \\ + d_\omega^H \cdot (\omega - \omega_0) + d_y^H \cdot (y - y_0).\end{aligned} \tag{1}$$

where coefficients d_Q^H, d_Q^H, d_ω^H are the partial derivatives of $H_t(Q_t, \omega, y)$ calculated at an operating point Q_{t_0}, ω_0, y_0. These coefficients are computed numerically by differentiating the head characteristic as:

$$d_Q^H := \left.\frac{\partial H_t}{\partial Q_t}\right|_{Q_{t_0}} = \frac{H_t(Q_{t_0} + \epsilon) - H_t(Q_{t_0} - \epsilon)}{2\epsilon}, \tag{2a}$$

$$d_\omega^H := \left.\frac{\partial H_t}{\partial \omega}\right|_{\omega_0} = \frac{H_t(\omega_0 + \epsilon) - H_t(\omega_0 - \epsilon)}{2\epsilon}, \tag{2b}$$

$$d_y^H := \left.\frac{\partial H_t}{\partial y}\right|_{y_0} = \frac{H_t(y_0 + \epsilon) - H_t(y_0 - \epsilon)}{2\epsilon}, \tag{2c}$$

where constant quantities have been omitted from the argument list for compactness. After linearizing as in (1), the model in Fig.3 becomes linear and time invariant. It can be expressed as a discrete-time state-space model and used in an MPC problem, as it will be described in the next section.

For the turbine's torque, a linearized model similar to the one of the head can be derived [12]:

$$\begin{aligned}\widetilde{T}_t(Q_t, \omega, y) \approx T_t(Q_{t_0}, \omega_0, y_0) + d_Q^T \cdot (Q_t - Q_{t_0}) + \\ + d_\omega^T \cdot (\omega - \omega_0) + d_y^T \cdot (y - y_0),\end{aligned} \tag{3}$$

[1]For the penstock, the resistance to the flow R depends on the flow rate Q_i; because the latter is a component of the model state, the formulation is bilinear (thus nonlinear).

where coefficients d_Q^T, d_Q^T, d_ω^T are obtained from the torque characteristics with the same numerical differentiation as in (2).

C. MPC for fatigue reduction

This section summarizes the method from [6], which is extended in the next section to include a BESS. The principle that the MPC leverages to limit the penstock's fatigue is a property of the Wohler's curve ([2]) of ferrous materials according to which cycles below a certain value, called *fatigue limit* and denoted by $\overline{\Delta\sigma}$, do not count towards accumulating fatigue [6], [13]. In other words, alternating forces acting on a component will not significantly impact its residual service life if these forces are small enough.

As it will be now described, by leveraging the linearized HPP presented in the former section, we infer the head, thus the force, and ultimately the stress (more formally, *hoop stress*, e.g. [14]) at the various sections of the penstock. Then, we require the hoop stress to undergo smaller variations than the fatigue limit to attain long life.

Let index t denote a time interval, and $h_i(t, y(t))$ denote the head at the portion i of the penstock at time interval t as a function of the guide vane $y(t)$. It is computed with the discrete state-space model of the linearized equivalent circuit described in the former section. For compactness, it is denoted by:

$$h_i(t, y(t)) = f_i(t, y(t)) \tag{4}$$

where f_i is a linear function. For an open-air penstock, the hoop stress $\sigma_i(t)$ (in Pascal) can be estimated as a function of the head as (e.g., [2], [15]):

$$\sigma_i(h_i(t, y(t))) = [h_i\,(t, y(t)) - z_i] \cdot \frac{kD}{2e} \quad i = 1, \ldots, \mathcal{I} \tag{5}$$

where z_i is the elevation at i, D and e are the penstock diameter and wall thickness, respectively, and $k = g\rho$ converts from head to pressure, with g acceleration of gravity and ρ water density. Say σ_{nom} is the nominal hoop stress at plant's steady state. It is easy to see that if the following inequality hold for all time intervals

$$\sigma_{\text{nom}} - \frac{\overline{\Delta\sigma}}{2} \leq \sigma_i(h_i(t, y(t))) \leq \sigma_{\text{nom}} + \frac{\overline{\Delta\sigma}}{2}, \tag{6}$$

then the maximum stress variation that can occur over time is the difference between the upper bound and the lower bound of (6), which corresponds to $\overline{\Delta\sigma}$, that is the fatigue limit.

The MPC problem for fatigue reduction consists in finding a new guide vane set point, denoted by $y^\dagger(t)$, that respects the constraint in (6). In order to attain the original regulation duties of the HPP on a best effort basis, we require $y^\dagger(t)$ to track as close as possible the original guide vane $y^\star(t)$. We do so by customarily minimizing the squared deviation between $y^\dagger(t)$ and $y^\star(t)$. These two elements (stress constraint and cost function) constitute the building blocks of the optimization problem underlying MPC.

Because f_i in (4) is a dynamic function of the guide vane (in the sense that it is derived from ordinary differential equations) and a control action at the current time will impact future penstock's heads, the MPC needs to implement a prediction horizon to ensure the penstock constraints to be respected during transients. The length of this prediction horizon, denoted by Γ (in number of samples), can be formally computed by considering either the transients' duration (or system eigenvalues) or the wave speed and the penstock length. Let τ denote the current time interval; the formulation of the optimization problem underlying MPC is:

$$\boldsymbol{y}^\dagger = \underset{\boldsymbol{y} \in \mathbb{R}^{\Gamma+1}}{\arg\min} \left\{ \sum_{t=0}^{\Gamma} \left(y(t) - y^\star(\tau + t)\right)^2 \right\} \tag{7a}$$

subject to guide vane limits for all time intervals

$$0 \leq y(t) \leq 1, \qquad t = 0, \ldots, \Gamma \tag{7b}$$

and penstock model and stress constraints for all time intervals and penstock elements:

$$h_i(t) = f_i(t, y(t)), \qquad t = 0, \ldots, \Gamma, \quad i = 1, \ldots, \mathcal{I} \tag{7c}$$

$$\underline{h} \leq h_i(t) \leq \overline{h}, \qquad t = 0, \ldots, \Gamma \quad i = 1, \ldots, \mathcal{I} \tag{7d}$$

where parameters $\underline{h}, \overline{h}$ are head limits given by combining (5) and (6). By virtue of the linearized models of the plant, Eq. (7d) is linear, resulting in a convex and tractable formulation of the optimization problem.

It is worth remarking that in (7a), future guide vane setpoints $\{y^\star(\tau + t),\ t = 0, \ldots, \Gamma\}$, necessary to compute the cost function , are unknown because they depends on future grid frequency conditions. We propose to estimate them with a persistent predictor, where future values match the current one. This strategy is effective already for fatigue reduction, as it will be shown in the results.

The optimization problem (7) is applied in a receding horizon fashion, i.e., solved at each time interval with updated information; only the first element of the decision vector $\boldsymbol{y}^\dagger$ is applied. The linear models can be recomputed when the plant's conditions change from the original linearization point.

In summary, this MPC provides a formal way to detect guide vane setpoint cycles that might harm the penstock. The guide vane setpoint computed by this MPC has the property of respecting the fatigue limit of the penstock, increasing its service life. By combining the original guide vane setpoint and the MPC one, one can derive the missing regulation of the HPP, which can be compensated for by using the BESS. This is the main principle of the proposed splitting policy and is described in the next section.

D. Computing the BESS power setpoint

The proposed controller filters the HPP's guide vane setpoint with the MPC described above, and then it uses the battery to provide the missing regulating power from the HPP compared to the original guide vane setpoint. This action

[2]The Wohler's curve, or SN curve, is an empirical relation that expresses the number of cycles N that a component can endure as a function of the stress variation that it undergoes.

preserves the original regulation commitment of the HPP while reducing penstock fatigue.

In this context, a straightforward way to understand the BESS power setpoint is as a difference between the power output that the HPP should have delivered with the original guide vane setpoint and the one implemented after the filtering action of the MPC. By denoting with $B^\dagger(t)$ the BESS power output at time t, this requirement can be formalized as:

$$B^\dagger(t) = P^\star(t) - P^\dagger(t), \tag{8}$$

where $P^\star(t)$ and $P^\dagger(t)$ correspond to the HPP's power output with the original guide vane $y^\star$ and modified guide from the MPC $y^\dagger$, respectively.

However, while the latter quantity could be accessed, e.g., from measurements because it is physically realized, the former power output is not available because it is unrealized, being the original control setpoint never implemented. This limitation makes the computation of (8) as a difference of two observed quantities not practicable in real life. To solve this problem, we propose to estimate the unrealized power output with an estimation model, an example of which is explained in the following.

1) Modeling the unobserved HPP production: As stated earlier, $P^\star$ is not available from measurements because it is unrealized, being the control action without MPC never actuated. As a first approximation, we propose to estimate it as (with the $\hat{\cdot}$ notation referring to estimated quantities, as opposed to measured ones):

$$\hat{P}^\star(t) = \hat{T}^\star(t) \cdot \hat{\omega}^\star(t) \tag{9}$$

where $\hat{T}^\star$ and $\hat{\omega}^\star$ are the hydraulic turbine's estimated torque and angular velocity the original guide vane setpoint $y^\star$. Because the frequency in power grids is regulated to a nominal value (e.g., 50 Hz) and we consider a small signal context for this control model where variations are small within a control cycle with linearization recomputed for new conditions, we assume the grid frequency to be constant and the generator synchronized to the grid, yielding the following approximation:

$$\hat{P}^\star(t) = \hat{T}^\star(t) \cdot 2\pi \cdot \frac{f_o}{\rho} \tag{10}$$

where f_o is the nominal grid frequency and ρ the polar couples of the electric generator. The modeling approximations and assumptions introduced in this section for the MPC (in particular, linear model, constant grid frequency, and synchronized generator) are validated in the results against more complete simulation models, including swing equation and generator models.

Being the angular velocity of the generator approximated to a constant, the problem of estimating the HPP power in (9) reduces to estimating the torque of the hydraulic turbine in (10). To estimate the torque, we propose to use the linearized model introduced in (3) from [12]. For convenience in the following formulation, the linear estimation model of the torque as a function of the guide vane is denoted by the function $z(y(t))$ (other model parameters and variables are not reported for simplicity). With this notation, the estimated power in (9) can be written as:

$$\hat{P}^\star(t) = z(y^\star(t)) \cdot 2\pi \cdot \frac{f_o}{\rho}. \tag{11}$$

E. Computing the battery power setpoint

Eq. (11) can be now used to estimate the first term on the right-hand side of (8). The second term, $P^\dagger_{\text{HPP}}(t)$, could be from measurements: this comes at the price of accepting a delay because the plant's power output for the currently implemented guide vane $y^\dagger(t)$ is not available just yet. Instead of a delayed measurement, one can use the same approach seen for (11) and estimate it. This reads as:

$$\hat{P}^\dagger(t) = z(y^\dagger(t)) \cdot 2\pi \cdot \frac{f_o}{\rho}. \tag{12}$$

By combining (8), (11), and (12), the BESS setpoint finally reads as:

$$B^\dagger(t) = \left[z(y^\star(t)) - z(y^\dagger(t))\right] \cdot 2\pi \cdot \frac{f_o}{\rho}, \tag{13}$$

thus proportional to the difference between the linear estimates of the torques under the original and filtered guide vanes. Compared to using delayed measurements, the method in (13) has the advantage that if the two guide vane setpoints are reasonably similar (as we would expect in a small signal context), the modeling error of the linear torque model $z(\cdot)$ cancels out.

F. Hybrid controller

Several ways are possible to combine the MPC for fatigue reduction in (7) with the BESS injection model (13), including augmenting the formulation of the MPC with new constraints to model the BESS injections and its constraints.

However, at the current stage we opt for a simpler and more interpretable hierarchical strategy, which is now described. At each time interval:

1) the linearized models f and z for penstock head and turbine torque are computed using recent measurements;
2) the MPC problem in (7) is solved as a function of the plant model f and using the target guide vane $y^\star$ from the governor as an input to the problem, making available $y^\dagger$ for the current time interval;
3) $y^\star$, $y^\dagger$ and the turbine torque model z are used to compute the BESS injection with (13).

The BESS injection should be properly adjusted to ensure that it respects the four-quadrant power converter (e.g. [16]) and battery operational constraints. These requirements, along with the reactive power contribution of the power converter and energy management of the battery system, are neglected at the current stage because we are interested in evaluating the global BESS power injection and comparing it with the power output of the HPP to quantify the extent of the required BESS power.

It is worth highlighting that because of the hierarchical structure of the controller, the linearity of the models involved

in (13) is not a strict requirement for the tractability of the problem as this would not impact on the convexity of the MPC. Because of this, more complex simulation models or digital twins (e.g., [17]) can be used to replace the linear estimates of the turbine's speed and torque, and HPP power.

IV. Results and Discussion

This section aims at illustrating the operations of a conventional HPP compared to its hybrid counterpart. The comparison involves evaluating the fatigue incurred by the penstock and the power output of the various components.

A. Case Study

The case study is a 230 MW medium-head HPP. It has a net head of 315 meters, one Francis turbine, and an open-air 1'100 meter-long penstock. Model attributes are summarized in Table I for reproducibility. The plant is equipped with a standard governor that includes a proportional-integral (PI) regulator with a speed droop and setpoint for speed-changer setting. The PI gains are determined with the Ziegler-Nicholas method. Parameters and model performance is validated by verifying the ENTSOE qualification tests for PFR [18], [19]. The regulator implements limits for the rate-of-change and magnitude of the guide vane actuator [18]. The permanent speed droop is set to 2%. Compared to conventional speed droops for HPPs that are between 2.5% and 5%, we choose a lower value to reproduce future operational settings where larger support might be required from dispatchable resources.

The plant simulates primary frequency regulation using a grid frequency signal from the low-inertia power system in [20] to reproduce conditions that might happen in future grid scenarios. It is worth highlighting that the utility of the proposed model is not limited to primary frequency regulation but, more in general, to dynamics related to any change of setpoints (e.g., secondary frequency control, rescheduling). For example, it was demonstrated in [2] that secondary frequency regulation leads to more severe penstock damages than primary control. Inclusions of setpoints from secondary frequency control will be considered in future works.

Since, at this stage, we are interested in evaluating the share of total power that the BESS takes as a function of the HPP's limitations, we assume that that the BESS power converter rating is large enough to accommodate any BESS setpoint request. In other words, we assume that BESS constraints in the MPC splitting problem are not binding. It is to note that, since the converter power rating and BESS energy capacity are linked by the C-rate specs of the battery cells (i.e., maximum charging or discharging current [A]/battery capacity [Ah]), we also assume that the BESS energy capacity is large enough to accommodate the required power setpoint. This modeling choice is because it enables a preliminary evaluation of the BESS's sizing requirements compared to the plant's total power.

TABLE I
Parameters of the HPP case study

Parameter	Unit	Value
Nominal power	MW	230
Nominal head	m	315
Nominal discharge	m^3/s	85.3
Nominal speed	rpm	375
Nominal torque	Nm	5.86×10^6
Length of penstock	m	1'100
Diameter of penstock	m	5
Wave speed	m/s	1'100

B. Control and simulation models

Control models are computed with the linearized models and assumptions described in Section III. Simulations are performed using more realistic and nonlinear simulation models, described here, to assess the extent of the modeling errors and the accuracy of the control action in a more realistic context. In the rest of this section, outputs of the nonlinear models are sometimes referred to as ground-truth values to denote that they represent the benchmark values.

The HPP is modeled with the nonlinear model discussed in III-A. The penstock is discretized with 20 elements, which are sufficient to represent the hydraulic transients accurately. The hydraulic turbine is modeled with the nonlinear head and torque characteristics. The power grid is modeled as an infinite bus, where the power grid imposes the grid frequency under the assumption that its size is significantly larger than the simulated plant. The generator is modeled with a quasi-static model that includes the swing equation (with the moment of inertia given by combining all the rotating masses); the power transfer between the power plant and the grid is modeled with the power-angle model. The model is simulated in MATLAB with an integration time of 4 ms. The MPC action is re-actuated each 50 ms.

The BESS is modeled as a power source. Due to the lack of mechanical time constants and extremely high ramping rates of BESS, it is assumed that BESS can implement setpoints within a single MPC cycle. BESS efficiency is considered ideal as energy losses are of limited interest for the moment.

C. Results

Simulations are one day long and refer to a case where the HPP provides primary frequency regulation to the grid. Results are reported only for a small period of the simulation interval for a reason of space, but conclusions extend to the whole period equally.

The upper panel of Fig. 4 shows the guide vane setpoint of the standard governor and the one of the MPC. As visible, these two setpoints are the same most of the time. This fact is to be expected and follows from the requirement that the MPC should provide the same regulation duties as the original governor. As explained above, this requirement is achieved by minimizing the norm-2 between the governor guide vane and the MPC one subject to constraints, resulting in identical guide vanes when constraints are not active. However, it is possible to see that when the governor's guide vane violates

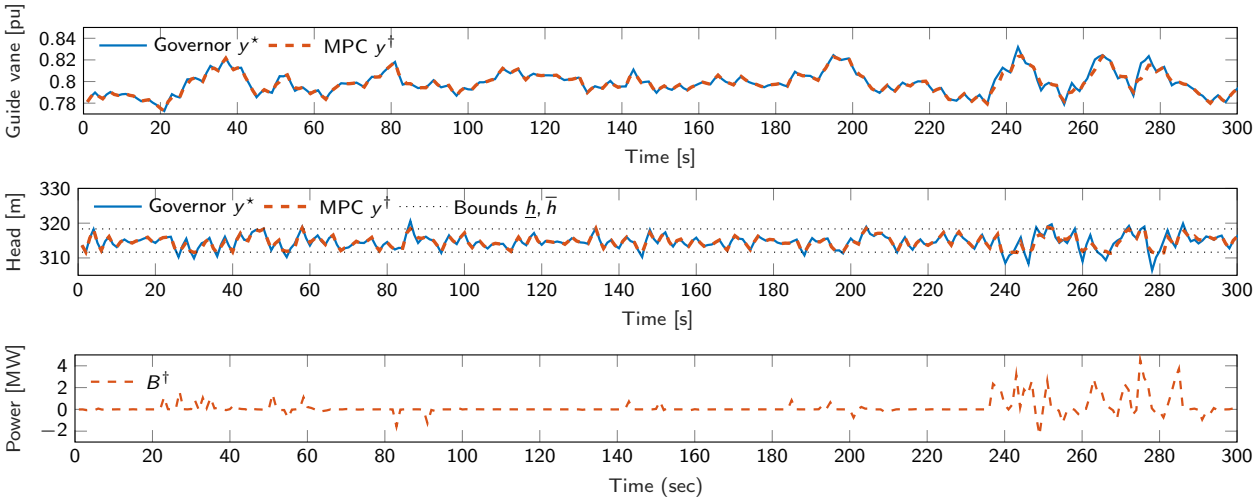

Fig. 4. Governor guide vane versus the MPC one (in the upper panel), head of the penstock's critical element under governor and MPC control and head constraints (middle panel), battery power (lower panel).

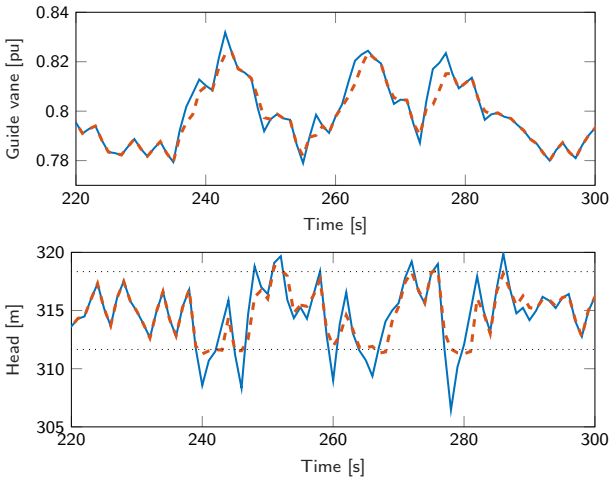

Fig. 5. A zoomed view of Fig. 4 (line styles and colors are the same as there). When the head limits are violated (bottom panel), the MPC corrects the guide vane (upper panel) so as to respect them.

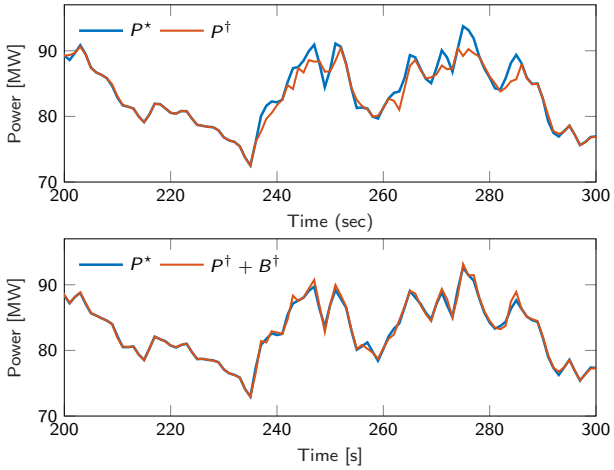

Fig. 6. A comparison of the power output of the HPP with the original guide vane, $P^\star$, of the HPP under MPC control, $P^\dagger$, and finally of the hybrid power plant, $P^\dagger + B^\dagger$.

the head limits and constraints become active (plot in the middle panel of Fig. 4), the MPC produces a setpoint that differs from the original one. This control action ultimately ensures the penstock head to stay within the prescribed limits. Finally, the plot in the lower panel of Fig. 4, shows the BESS contributions. As to be expected from the formulation, the BESS operates only when the head constraints are active. It is noteworthy that the BESS power is a few MWs, compared to a plant's power output of around 80 MW (as shown later). This denotes that a small battery injection is sufficient to attain problem targets. Implications on the required BESS energy capacity and rated power will be investigated in future works.

Fig. 5 shows a zoomed view of the guide vanes and head constraint (lines' colors and styles have the same meaning as in Fig. 4). The top panel of Fig. 5 shows that the MPC action resembles the one of a rate limiter, however activated only when variations of guide vane are large. As visible from the bottom panel plot of Fig. 5, the head after the MPC action (dashed line) presents marginal violations of the head constraints: these are due to the estimation error of the head linear model.

Fig. 6 shows the power output of three cases: when the HPP is operated with the original guide vane setpoint ($P^\star$), when the HPP is operated with the MPC ($P^\dagger$), and ultimately the power output of the hybrid plant, given by the sum of the HPP's and BESS's contributions ($P^\dagger + B^\dagger$). $P^\star$ is intended as a reference for the regulating power that the HPP should have provided in the original setting. It is possible to see that, while the HPP under MPC control does not track the reference power output (thus not providing the same regulating power), the hybrid plant closely tracks it. We can thus conclude that the requirement of controlling the battery so that the hybrid HPP

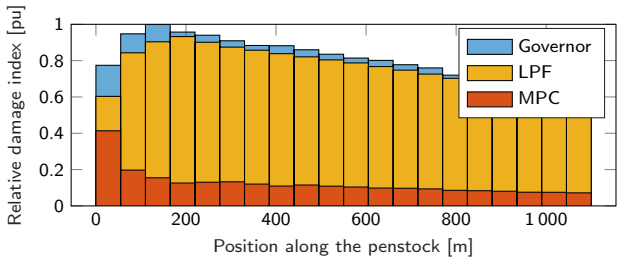

Fig. 7. Relative cumulative damage index along the penstock with reference to the case without filtering in hybrid mode with MPC and low-pass filter.

attains the same power regulation capability as the original HPP is met.

The impact on penstock service life is now discussed. Fig. 7 shows the relative damage index along the penstock (0 m refers to the part of the penstock at a higher altitude, and viceversa). The relative damaged index is defined as the damage index divided the largest damage index observed across all cases. The damage index is computed as described in [2], [21]. Briefly, it consists in calculating the head and stress in each penstock element; then, a rain-flow counting is used to count stress cycles at various stress intensity variations; finally, based on these information and as a function of a given Wohler's curve, the Miner rule is applied to compute the damage index. From Fig. 7, it can be seen that the MPC achieves a smaller damage compared to the standard governor. It can be concluded that the hybrid controller achieves to deliver the same regulating power (Fig. 6) at a fraction of the damage.

Fig. 7 also shows a comparison against the splitting problem solved with a low-pass filter (LPF). Its cut-off frequency (1.46 Hz) is chosen to deliver *similar* regulating power to the grid as the MPC (to enable a fair comparison). Similarity is measured in terms of correlation coefficient between the power output and the grid frequency signal. It is found that the MPC performs better than the LPF, and that the latter used the BESS more than the former (not shown here for a reason of space).

V. Conclusions

This paper has described a model predictive control (MPC) for hybrid HPP to attain penstock's fatigue reduction in medium- and high-head plants. The power setpoint splitting strategy for the hydraulic turbine and BESS relies on an explicit formulation of the mechanical loads incurred by the HPP's penstock, which can be damaged due to fatigue when providing regulating power to the grid. By removing those components conducive to excess penstock fatigue from the HPP power setpoint and adequately controlling the BESS, the proposed MPC could deliver similar regulating power as the original HPP while significantly decreasing damages to the hydraulic conduits. Simulations were performed considering a 230 MW medium-head hydropower plant. It was observed that the BESS power contribution necessary to reduce penstock fatigue was a small fraction of the rated power, with possible positive implications for BESS sizing's requirements and degradation, which will be investigated in future works.

References

[1] IEA, "Hydropower special market report, IEA," Paris, Tech. Rep., 2021. [Online]. Available: https://www.iea.org/reports/hydropower-special-market-report

[2] M. Dreyer, C. Nicolet, A. Gaspoz, D. Biner, S. Rey-Mermet, C. Saillen, and B. Boulicaut, "Digital clone for penstock fatigue monitoring," in *IOP Conference Series: Earth and Environmental Science*, vol. 405, no. 1. IOP Publishing, 2019.

[3] F. Gerini, E. Vagnoni, R. Cherkaoui, and M. Paolone, "Improving frequency containment reserve provision in run-of-river hydropower plants," *Sustainable Energy, Grids and Networks*, vol. 28, 2021.

[4] W. Yang, P. Norrlund, L. Saarinen, J. Yang, W. Zeng, and U. Lundin, "Wear reduction for hydropower turbines considering frequency quality of power systems: A study on controller filters," *IEEE Transactions on Power Systems*, vol. 32, no. 2, 2017.

[5] C. Jin, N. Lu, S. Lu, Y. Makarov, and R. A. Dougal, "Coordinated control algorithm for hybrid energy storage systems," in *2011 IEEE Power and Energy Society General Meeting*, 2011, pp. 1–7.

[6] S. Cassano and F. Sossan, "Stress-informed control of medium- and high-head hydropower plants to reduce penstock fatigue," *Sustainable Energy, Grids and Networks*, vol. 31, p. 100688, 2022.

[7] B. Xu, A. Oudalov, J. Poland, A. Ulbig, and G. Andersson, "Bess control strategies for participating in grid frequency regulation," *IFAC Proceedings Volumes*, vol. 47, no. 3, pp. 4024–4029, 2014.

[8] E. Namor, D. Torregrossa, F. Sossan, R. Cherkaoui, and M. Paolone, "Assessment of battery ageing and implementation of an ageing aware control strategy for a load leveling application of a lithium titanate battery energy storage system," in *2016 IEEE 17th Workshop on Control and Modeling for Power Electronics (COMPEL)*. IEEE, 2016, pp. 1–6.

[9] O. Jr, N. Barbieri, and A. Santos, "Study of hydraulic transients in hydropower plants through simulation of nonlinear model of penstock and hydraulic turbine model," *IEEE Transactions on Power Systems*, vol. 14, 12 1999.

[10] L. C. Evans, *Partial differential equations*, ser. Graduate studies in mathematics. Providence, R.I: American Mathematical Society, 1998, no. v. 19.

[11] C. Nicolet, "Hydroacoustic modelling and numerical simulation of unsteady operation of hydroelectric systems," Ph.D. dissertation, EPFL, Lausanne, 2007.

[12] S. Cassano, F. Sossan, C. Landry, and C. Nicolet, "Performance assessment of linear models of hydropower plants," in *2021 IEEE PES Innovative Smart Grid Technologies Europe (ISGT Europe)*, 2021.

[13] I. Hadley, "Bs 7910:2013 in brief," *International Journal of Pressure Vessels and Piping*, vol. 165, 2018.

[14] E. B. Wylie, V. L. Streeter, and L. Suo, *Fluid transients in systems*. Prentice Hall Englewood Cliffs, NJ, 1993, vol. 1.

[15] A. Pachoud, R. Berthod, P. Manso, and A. Schleiss, "Advanced models for stress evaluation and safety assessment in steel-lined pressure tunnels," *International Journal on Hydropower and Dams*, 09 2018.

[16] A. Zecchino, Z. Yuan, F. Sossan, R. Cherkaoui, and M. Paolone, "Optimal provision of concurrent primary frequency and local voltage control from a BESS considering variable capability curves: Modelling and experimental assessment," *Electric Power Systems Research*, vol. 190, p. 106643, 2021.

[17] C. Nicolet, M. Dreyer, A. Beguin, E. Bollaert, S. Torrent, and J. Dayer, "Hydraulic transient survey at cleuson-dixence with real-time hydroclone monitoring system," in *Proc. of HYDRO 2018 Conference*, 2018.

[18] C. Landry, C. Nicolet, J. Gomes, and F. Avellan, "Methodology to determine the parameters of the hydraulic turbine governor for primary control," Power Vision Engineering, Tech. Rep., 2019.

[19] M. Scherer, D. Schlipf, and W. Sattinger, "Test for primary control capability," Internet Requests for Comments, Swissgrid, RFC, 2011.

[20] Y. Zuo, Z. Yuan, F. Sossan, A. Zecchino, R. Cherkaoui, and M. Paolone, "Performance assessment of grid-forming and grid-following converter-interfaced battery energy storage systems on frequency regulation in low-inertia power grids," *Sustainable Energy, Grids and Networks*, vol. 27, p. 100496, 2021.

[21] S. Cassano, C. Nicolet, and F. Sossan, "Reduction of penstock fatigue in a medium-head hydropower plant providing primary frequency control," in *2020 55th International Universities Power Engineering Conference (UPEC)*. IEEE, 2020, pp. 1–6.